Available online at www.sciencedirect.com
ScienceDirect
Ceramics International 38S (2012) S343–S346
CERAMICS INTERNATIONAL
www.elsevier.com/locate/ceramint

Crystal phases and electric properties of $(Na_{0.5}K_{0.5})_{1-x}Nb_{1+x/5}O_3$:$y$CuO, zLiSbO$_3$ piezoceramics

S.H. Moon [a], S.H. Han [b], H.W. Kang [b], H.-G. Lee [b], K.W. Chae [c], J.S. Kim [a,*], C.I. Cheon [a,c]

[a] Department of Semiconductor & Display Engineering, Hoseo University, Chungnam 336-795, Republic of Korea
[b] Electronic Materials and Device Research Center, Korea Electronics Technology Institute, Kyeonggi 463-816, Republic of Korea
[c] Department of Materials Science & Engineering, Hoseo University, Republic of Korea

Available online 5 May 2011

Abstract

In this study the electric property and the formation of crystal phases are characterized along with the increase of the A-site alkali deficiency(x) in the non-stoichiometric $(Na_{0.5}K_{0.5})_{1-x}Nb_{1+x/5}O_3$:$y$CuO + zLiSbO$_3$ ($x = -0.01$ to 0.1; $y = 0, 0.01$; $z = 0, 0.05$) ceramics. Quantitative crystal phase analysis has been carried out using Rietveld method. The crystal structure of tetragonal tungstenbronze phase is discussed in relation with the P–E hysteresis and dielectric properties. The stoichiometric and the slightly alkali deficient samples show very leaky P–E loop. With increasing the alkali deficiency the electrical leakage decreases and the P–E loop shows the saturation. CuO and LiSbO$_3$ doping in the alkali deficient sample ($x = 0.05$, $y = 0.01$, $z = 0$) leads to the slim and pinched P–E loop shape. By CuO doping the P_r and P_s decreases to 13.9 and 20.87 μC/cm^2 from 25.6 and 27.2 μC/cm^2, respectively.

Keywords: A. Sintering; C. Ferroelectric properties; Potassium sodium niobate; Tetragonal tungstenbronze

1. Introduction

Lead-free piezoelectric ceramics based on (Na,K)NbO$_3$ (NKN) show the best piezoelectric properties among the several alternative candidates [1–3]. For preparing NKN ceramics with superior piezoelectric properties, deliberate controls over the sintering conditions, additives, and compositions have been important issues during the last several years [4–6].

Volatilization of alkali elements is critically detrimental to both the sintered density and the piezoelectric properties in the NKN ceramics [7]. Contrarily to these common knowledge, a few previous reports suggested that A-site deficient NKN ceramics can be sintered at atmospheric pressure to a very high density (4.4 g/cm^3) which is comparable to that of hot-pressed NKN (4.46 g/cm^3) [8,9]. Initially the A-site deficient NKN having a superior piezoelectric property ($k_p = 0.41$, $Q_m = 1400$) has been reported by Matsubara et al. [8] for the $(Na_{0.5}K_{0.5})_{0.97}(Nb_{0.95}Ta_{0.05})O_3$:0.04CuO. Similarly Rubio-Marcos et al. [9] also reported a superior piezoelectric property ($T_c \approx 250$ °C, $d_{33} \approx 300$ pC/N) for the A-site deficient $(Na_{0.52}K_{0.44}Li_{0.04})(Nb_{0.86}Ta_{0.10}Sb_{0.04})O_3$ ceramic. In these two reports the formation of tetragonal tungstenbronze phase (TTP) was observed as a second phase. This phase was indexed as $K_4CuNb_8O_{23}$ (JCPDS 41-0482) and $K_3LiNb_6O_{17}$(JCPDS 36-0533), respectively. This TTP was ascribed to the origin of the high density and superior piezoelectric property due to a low sintering temperature of 1000 °C and relatively high dielectric constant ($\varepsilon_r \approx 250$).

The TTP has not been known much of its correct composition nor the crystal structure. For example, the composition of the TTP in the previous two papers is different from each other. Moreover, a similar TTP has often been observed even in the $(Na_{0.5}K_{0.5})NbO_3$ without any additives which were sintered at high temperature. In this study we investigated the crystal phases and electric properties of the non-stoichiometric compositions $(Na_{0.5}K_{0.5})_{1-x}Nb_{1+x/5}O_3$:$y$CuO + zLiSbO$_3$ ($x = -0.01$ to 0.1; $y = 0$, 0.01; $z = 0$, 0.05) ceramics. Along with the increase of the alkali deficiency(x) in A-site, the P–E hysteresis, sintered density, and the evolution of crystal phases are characterized. Quantitative amount of the orthorhombic *Amm*2, tetragonal *P*4*mm*, and TTP phases

* Corresponding author. Tel.: +82 41 5405921; fax: +82 41 5405929.
E-mail address: kimjungs@hoseo.edu (J.S. Kim).

0272-8842/$36.00
doi:10.1016/j.ceramint.2011.04.116

are analyzed using Rietveld refinement method. The correct crystal structure of TTP is presented in this study.

2. Experimental

Non-stoichiometric samples with CuO and $LiSbO_3$ additives were prepared using a conventional solid state process. The nominal composition of the samples is represented as $(Na_{0.5}K_{0.5})_{1-x}Nb_{1+x/5}O_3$:$y$CuO + zLiSbO$_3$ ($x = 0.0$, 0.002, 0.05, 0.1; $y = 0$, 0.01; $z = 0$, 0.05). The starting materials were K_2CO_3, Na_2CO_3, Li_2CO_3, Nb_2O_5, Sb_2O_5 and CuO. The starting materials were weighed appropriately according to the desired compositions and were ball milled in ethanol for 24 h. After ball milling the mixture was calcined at 600 °C for 5 h. The calcined powder was ball milled with PVA binder in ethanol for 24 h. After drying the powder mixture was compacted into disc of 10 mm dia. × 1 mm thickness. The compacted sample was heat treated at atmospheric pressure and at the temperatures ranging from 1080 °C to 1100 °C for 3 h.

Hysteresis curves of polarization–electric field (P–E) at RT have been measured using RT66A ferroelectric tester of Radiant Technologies. The X-ray diffraction data were obtained at room temperature using a D/max-RC diffractometer with Cu Kα in the 2θ range of 10–100°. The crystal structure was analyzed by the Rietveld profile refinement method using a version 3.2 of the program Fullprof.

3. Results and discussion

In NKN ceramics the orthorhombic (*Amm*2) and the tetragonal (*P*4*mm*) phases usually coexists. In alkali deficient samples the TTP (*P*4/*mbm*) also coexists and the diffraction peaks from the TTP heavily overlap with those of the perovskite phases, *Amm*2 and *P*4*mm*. In this study, quantitative amount of the coexisting phases are analyzed by Rietveld method using the structural model of the three phase mixture, *Amm*2, *P*4*mm*, and *P*4/*mbm*. When the three phase model was adopted, we obtained the low enough *R*-values (R_p: 8.0–11.0, R_b: 2.3–4.4, R_f: 1.8–2.8). Crystal phases, unit cell volumes, and vol.% of each crystal phase are summarized in Table 1 for the A-site deficient samples $(1-x)(Na_{0.5}K_{0.5})Nb_{1+x/5}O_3 + y$CuO + zLiSbO$_3$. The Rietveld refinement show the lattice parameters of the constituent phases as follows.

Table 1
Refinement results for $(1-x)(Na_{0.5}K_{0.5})Nb_{1+x/5}O_3 + y$CuO + zLiSbO$_3$ samples: unit cell volumes, vol.% of crystal phases, and *R*-values.

Space group	Sample compositions		
	$x = 0.05$, $y = z = 0.0$	$x = 0.05$, $y = 0.01$, $z = 0.05$	$x = 0.10$, $y = 0.01$, $z = 0$
Cell volume (Å^3)			
*Amm*2	126.04	125.69	125.78
*P*4*mm*	62.84	62.46	62.81
*P*4/*mbm*	624.06	624.71	624.62
Crystal phase (vol.%)			
*Amm*2	77.30	57.3	76.2
*P*4*mm*	19.3	39.4	16.6
*P*4/*mbm*	3.4	3.3	7.2

Orthorhombic : $a = 3.9397-3.9439$ Å, $b = 5.6345-5.6394$ Å, $c = 5.6562-5.6708$ Å

Tetragonal : $a = b = 3.9762-3.9818$ Å, $c = 3.9505-3.9677$ Å

TTP : $a = b = 12.5538-12.5644$ Å, $c = 3.9572-3.9608$ Å

Fig. 1(a) represents the refined profile pattern for the $(1-x)(Na_{0.5}K_{0.5})Nb_{1+x/5}O_3$:$y$CuO ($x = 0.1$, $y = 0.01$). The inset shows a refined profile zoomed in the $2\theta = 44.5$–47.5 range. In our samples the tetragonal phase constitutes a minor proportion of about 15.1–39.4 vol.% (Table 1). The 0.005 $LiSbO_3$-doped sample, $0.95(Na_{0.5}K_{0.5})Nb_{1.01}O_3$:0.01CuO + 0.05$LiSbO_3$, shows the highest tetragonal proportion of 39.4%. Without $LiSbO_3$ doping the proportions of the tetragonal phase is 15.1–24.1%. Small amount of TTP formed in every sample except the stoichiometry sample ($x = 0$). At the alkali deficiency of $x = 0.05$ the amount of TTP is 3.2–3.4 vol.%. When the deficiency × increase to 0.10, the amount of TTP is doubled (7.2 vol.%).

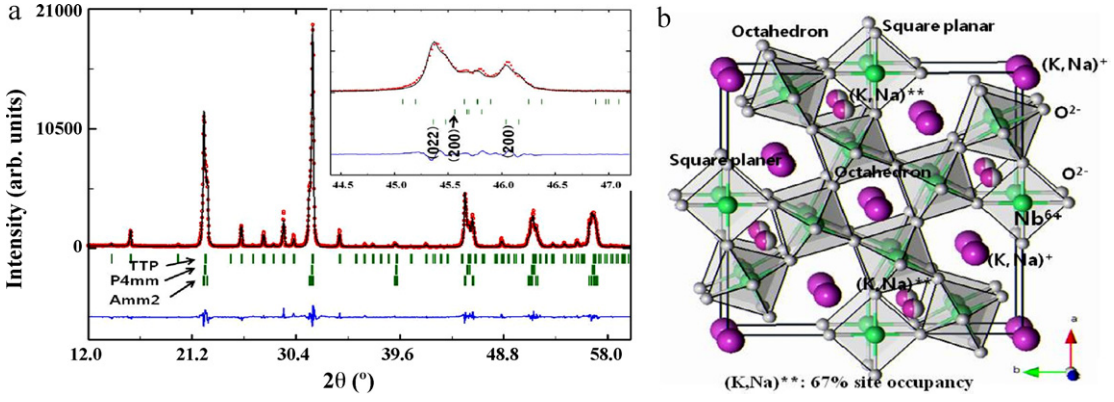

Fig. 1. (a) The refined profile pattern for the $(1-x)(Na_{0.5}K_{0.5})Nb_{1+x/5}O_3$:$y$CuO ($x = 0.1$, $y = 0.01$, $z = 0$) using the three phases (*Amm*2 + *P*4*mm* + *P*4/*mbm*) model. [Inset: refined profile zoomed in the $2\theta = 44.5$–47.5 range]. (b) Refined crystal structure of the TTP phase.

The refined crystal structure of the TTP phase (*P4/mbm* model) is represented in Fig. 1(b). This crystal structure is one of the tungsten bronze-types [10], and consists of 1 perovskite block, 4 pentagonal prism, and 4 trigonal prism blocks formed by the infinite Ti–O octahedron chains along the *c*-axis. The cation site in the trigonal prim marked as (Na, K)** represents ($Na_{0.5}K_{0.5}$) ion and has a partial occupancy of 67%.

Initially the TTP of *P4/mbm* space group was reported by Kumada et al. [11]. In his model the chemical formula was reported as $K_6Nb_{10.9}O_{30}$, which formula implies that the Nb^{6+} ion partially occupies (22%) the trigonal prism channel. But, our refinement results show that the $(Na,K)^{**}$–O average bond distance (in trigonal prism) is 2.45 Å. This bond distance is close to that of (Na,K)–O bonds (K1 = 2.98, K2 = 2.82 Å) not the Nb–O bonds (Nb1 = 1.98, Nb2 = 1.94 Å). By putting ($Na_{0.5}K_{0.5}$) ion at the trigonal prism site (K3) we got the site occupancy of 67%. The chemical formula deduced from this refinement results is $(Na_{0.5}K_{0.5})_{8.7}Nb_{10}O_{30-\delta}$. The doped ions Cu^{2+} and Li^{+} can substitute for the Nb-site and (Na,K) sites respectively in the TTP.

One of the characteristic features of the TTP is that the $d_{(h\ k\ l)}$ spacings of the TTP and the NKN phases are heavily overlapped each other (see Fig. 1(a)). This implies that TTP structure has substantially common features with the NKN. The *c*-axis of TTP corresponds to a single unit cell axis of the perovskite. Hence the c-axis parameter of TTP (3.973 Å) matches for the *a*-axis of NKN (3.998 Å). And (3 1 0), (4 2 0), and (3 1 1) in NKN match for the (0 1 1), (0 0 2), and (1 1 1) in TTP.

Fig. 2 shows the linear sintering shrinkage of the nonstoichiometric samples $(1-x)(Na_{0.5}K_{0.5})Nb_{1+x/5}O_3$ without additive ($x = -0.01$ to $+0.05$). Alkali excess samples show very poor sinterability. Contrarily with the increase of the alkali deficiency the sintering shrinkage increases at both 1080 °C and 1100 °C. Rubio-Marcos et al. [9] suggested that the low melting TTP leads to a transient liquid phase formation and the high sintering density in the (Na,K) deficient. However, the SEM images and the shape of the sintered sample do not indicate any evidence of liquid phase sintering even in the highest degree of (Na,K) deficient composition ($x = 0.1$, $y = 0.1$, $z = 0.0$). The enhancement of sinterability is ascribed to the sintering agent effect of TTP. Since the alkali deficient samples starts its consolidation process at low temperature (~1000 °C) [8], the alkali volatilization is suppressed. Hence the alkali deficient samples become highly sinterable. The other feature worthwhile to consider for the sinterability is the lattice matching between the TTP and NKN (Fig. 1). Lattice matching usually results in a low interfacial energy, and inhibit the grain boundary migration during sintering process.

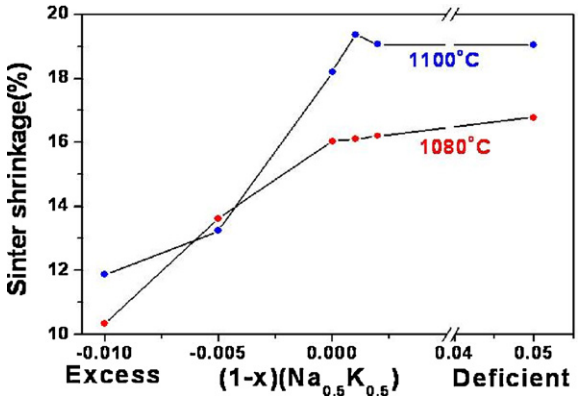

Fig. 2. Linear sintering shrinkage of the $(1-x)(Na_{0.5}K_{0.5})Nb_{1+x/5}O_3$ samples ($x = -0.1$ to $+0.05$) (-0.1, -0.05, 0.0, 0.001, 0.002, 0.05) without additive sintered at 1080 °C and 1100 °C for 3 h.

The P–E hysteresis loops of the stoichiometric and the slightly deficient samples $(1-x)(Na_{0.5}K_{0.5})Nb_{1+x/5}O_3$ ($x = 0.0$, $x = 0.001$, $y = z = 0$) show very leaky P–E loop shape. By increasing the deficiency to $x = 0.002$ and 0.05, we could increase the applied voltage up to 40 kV/cm and obtain a saturated P–E hysteresis. The electrical properties including P_r, P_s, E_c, and dielectric constant (ε_r) are summarized in Table 2.

Fig. 3 represents the P–E hysteresis loops for the samples $(1-x)(Na_{0.5}K_{0.5})Nb_{1+x/5}O_3$ $(1-x)(Na_{0.5}K_{0.5})Nb_{1+x/5}O_3$:$y$CuO + zLiSbO$_3$ which were sintered at 1080 °C for 3 h. The effect of the dopant and the degree of alkali deficiency on the P–E hysteresis can be found. The alkali deficient sample without dopant (A: $x = 0.5$, $y = z = 0.0$) shows the largest P_r and P_s values, 25.6 and 27.2 μC/cm^2. By CuO doping (B: $x = 0.05$, $y = 0.01$, $z = 0$) the P–E hysteresis loop becomes slim and pinched shape. The P_r and P_s decreases to 13.9 and 20.87 μC/cm^2, respectively. The E_c also decreases to 14.5 from 23.5 kV/cm. In our study the CuO doping produced the pinching-off effect of P–E hysteresis in addition to the sintering agent effect. The apparent decrease of polarization by CuO doping is mainly from a reduction of electrical leakage. The CuO in the PZT play an important role in the pinning of domain wall and in pinching the P–E hysteresis.

At the highest alkali deficiency ($x = 0.1$, $y = 0.01$, $z = 0.0$:C in Fig. 3) showing 7.2 vol.% PPT, the P_r and P_s reduces further to 7.5 and 12.8 μC/cm^2, respectively. The presence of a large

Table 2
Summary of the electrical properties including P_r(μC/cm^2), P_s(μC/cm^2), E_c(kV/cm), and dielectric constant (ε_r, at 100 kHz) for the $(1-x)(Na_{0.5}K_{0.5})Nb_{1+x/5}O_3 + y$CuO + zLiSbO$_3$ samples.

Compo-sition	$x = y = z = 0$[a]	$x = 0.002$, $y = z = 0$[a]	$x = 0.05$, $y = 0.01$, $z = 0$	$x = 0.05$, $y = 0.01$, $z = 0.05$	$x = 0.1$, $y = 0.01$, $z = 0$
P_r	Leaky P–E loop	26.6	13.9	4.2	7.5
P_s		28.1	20.9	11.7	12.8
E_c		21.7	14.5	15.7	18.5
ε_r	469	468	372	408	376
Tan δ	0.25	0.10	0.03	0.01	0.04

[a] Sintered at 1100 °C; others at 1080 °C.

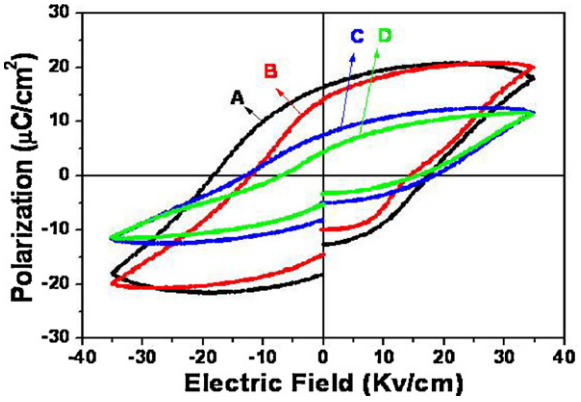

Fig. 3. P–E hysteresis loops of the $(1-x)(Na_{0.5}K_{0.5})Nb_{1+x/5}O_3$ $(1-x)(Na_{0.5}K_{0.5})Nb_{1+x/5}O_3$:$y$CuO + zLiSbO$_3$ samples sintered at 1080 °C for 3 h [A: no additive ($x = 0.05$, $y = z = 0.0$), B: 0.01 CuO doped ($x = 0.05$, $y = 0.01$, $z = 0.0$), C: 0.1 (Na,K) deficient and 0.01 CuO doped ($x = 0.10$, $y = 0.01$, $z = 0.0$), D: 0.05 LiSbO$_3$ doped ($x = 0.05$, $y = 0.01$, $z = 0.05$)].

amount TTP is believed to hinder the domain wall motion and lead to less saturation polarization. The co-doped sample with CuO and LiSbO$_3$ ($x = 0.05$, $y = 0.01$, $z = 0.05$: D in Fig. 3) shows the most severely pinched P–E hysteresis. In this co-doped sample the Li^+ ion is assumed to substitute for the A-site. Meanwhile the Cu^{2+} ion is assumed to substitute for the B-site in the perovskite based on the crystallographic aspects, i.e. the radius of Cu^{2+} (0.73 Å) and the oxygen coordination. Further works on the piezoelectric properties and the relation with the P–E pinch-off are necessary.

4. Conclusions

Alkali deficiency in non-doped NKN samples, $(1-x)(Na_{0.5}K_{0.5})Nb_{1+x/5}O_3$ leads to the formation of the tetragonal tungstenbronze phase (TTP, *P4/mbm*) as an impurity phase, of which phase the chemical formula is $(Na_{0.5}K_{0.5})_{8.7}Nb_{10}O_{30-\delta}$. The formation of TTP leads to higher sintered density than either the stoichiometric or alkali excess NKN sample. The alkali excess resulted in the very poor sintering shrinkage. Crystallographically TTP has common features with the NKN crystal structure that the $d_{(h\ k\ l)}$-spacings of the TTP are heavily overlapped with those of NKN phase. With increasing the alkali deficiency ($x = 0.002$, 0.05) the electrical leakage decreases and the P–E loop shows a saturation behavior. CuO doping in the alkali deficient sample ($x = 0.05$) makes the P–E hysteresis loop slim and pinched shape, and the P_r and P_s decreases to 13.9 and 20.87 μC/cm^2 from 25.6 and 27.2 μC/cm^2, respectively. Co-doping with both CuO and LiSbO$_3$ makes the P–E hysteresis heavily pinched shape.

Acknowledgements

This research was financially supported by a grant from the Fundamental R&D Program for Core Technology of Materials funded by the Ministry of Knowledge Economy, Republic of Korea.

References

[1] Y. Guo, K.-I. Kakimoto, H. Ohsato, Phase transitional behavior and piezoelectric properties of $(Na_{0.5}K_{0.5})NbO_3$–$LiNbO_3$ ceramics, Applied Physics Letters 85 (2004), 4124-1–4133-3.

[2] J. Rödel, W. Jo, K. Seifert, E. Anton, T. Granzow, D. Damjanovic, Perspective on the development of lead-free piezoceramics, Journal of the American Ceramic Society 92 (2009) 1153–1177.

[3] K. Wang, J.F. Li, N. Liu, Piezoelectric properties of low-temperature sintered Li-modified $(Na,K)NbO_3$ lead-free ceramics, Applied Physics Letters 93 (2008), 092904-1–92904-3.

[4] M. Kosec, D. Kolar, On activated sintering and electrical properties of $NaKNbO_3$, Materials Research Bulletin 10 (1975) 335–340.

[5] C. Lee, L. Wang, H.G. Yeo, J.H. Cho, Y.S. Sung, M.H. Kim, T.K. Song, S.S. Kim, B.C. Choi, Effects of A-site ionic contents on piezoelectric and ferroelectric properties of lead-free $(K_{0.5}Na_{0.5})NbO_3$–$LiNbO_3$ ceramics, Ferroelectrics 381 (2009) 176–180.

[6] J. Wu, D. Xiao, Y. Wang, J. Zhu, W. Shi, W. Wu, B. Zhang, J. Li, Phase structure, microstructure and ferroelectric properties of $(1-x)[(K_{0.50}Na_{0.50})_{0.94}Li_{0.06}]$ $(Nb_{0.94}Sb_{0.06})O_3$–xCaTiO$_3$ lead-free ceramics, Journal of Alloys and Compounds 476 (2009) 782–786.

[7] M.S Kim, D.S. Lee, E.C. Park, S.J. Jeong, J.S. Song, Effect of Na_2O additions on the sinterability and piezoelectric properties of lead-free $95(Na_{0.5}K_{0.5})NbO_3$–$5LiTaO_3$ ceramics, Journal of the European Ceramic Society 27 (2007) 4121–4124.

[8] M. Matsubara, W.T. Yamaguchi, W. Sakamoto, K. Kikuta, T. Yogo, S.I. Hirano, Processing and piezoelectric properties of lead-free (K,Na) (Nb,Ta) O_3 ceramics, Journal of the American Ceramic Society 88 (2005) 1190–1196.

[9] F. Rubio-Marcos, P. Marchet, T.M. Mejean, J.F. Fernandez, Role of sintering time, crystalline phases and symmetry in the piezoelectric properties of lead-free KNN-modified ceramics, Materials Chemistry and Physics 123 (2010) 91–97.

[10] J.S Kim, C.I. Cheon, T.R. Park, H.S. Shim, Dielectric properties and crystal structure of $Ba_{6-3x}(Nd, M)_{8+2x}Ti_{18}O_{54}$ (M = La, Bi, Y) microwave ceramics, Journal of Materials and Science 35 (2000) 1487–1494.

[11] N. Kumada, N. Kinomura, Preparation and crystal structure of $K_6Nb_{10.9}O_{30}$, European Journal of Solid State Inorganic Chemistry 34 (1997) 65–72.